Conductivity of tridecylmethylammonium-Au($dmit$)$_2$ Langmuir-Blodgett films under hydrostatic pressure

H. Isotalo and J. Paloheimo
VTT Electronics, Electronic Materials and Components, Technical Research Centre of Finland, Otakaari 7B, FIN-02150, Espoo, Finland

Y. F. Miura,* R. Azumi, M. Matsumoto, and T. Nakamura
National Institute for Materials and Chemical Research, 1-1 Higashi, Tsukuba, Ibaraki 305, Japan
(Received 22 July 1994)

The electrical conductivity of electrochemically oxidized Langmuir-Blodgett films of tridecylmethylammonium-Au($dmit$)$_2$ and icosanoic acid has been studied. The measurements were performed at temperatures down to 3 K and hydrostatic pressures up to 17 kbar, and also at high electric fields up to 3.2 kV/cm. The results support the view that the films consist of relatively large metallic islands, separated by thin barriers, and indicate that the low-temperature conductivity with $d\sigma/dT>0$ originates from thermal-fluctuation-induced tunneling. At higher temperatures $d\sigma/dT<0$ because of the finite resistance of the metallic islands. The conductivity increased upon applied pressure, and the temperature of the maximum conductivity shifted to lower temperature without any pronounced saturation. The ambient-pressure room-temperature conductivity of the best conducting samples could be increased by a factor of about 2 at 10-kbar hydrostatic pressure and further to 140 S/cm at the temperature of the maximum conductivity at 51 K.

I. INTRODUCTION

Measurements of the effect of hydrostatic pressure on the conductivity give important information concerning the charge-transport mechanisms. Especially interesting results have been obtained for organic charge-transfer complexes where pressure affects the intermolecular spacing and electronic structure, resulting in an increase of conductivity, a more metallic temperature dependence of conductivity, and, in favorable cases, in superconductivity. The pressure needed to reach the superconducting state varies from mild, ≈ 1 kbar, to moderate pressures, ≈ 20 kbar. For example, in the family of molecular charge-transfer salts formed with metal($dmit$)$_2$ ($dmit$ is 1,3-dithiol-2-thione-4,5-dithiolate) (TTF is tetrathiafulvalene) it was found that TTF[Ni($dmit$)$_2$]$_2$ becomes superconducting at 1.62 K under 7 kbar.[1] Later superconductivity was found in TTF[Pd($dmit$)$_2$]$_2$ ($T_c=6$ K at 19 kbar),[2] [$(CH_3)_4$N][Ni($dmit$)$_2$]$_2$ ($T_c=5$ K at 7 kbar),[3] and [$(CH_3)_4$N][Pd($dmit$)$_2$]$_2$ ($T_c=6.2$ K at 6.5 kbar).[4] On the other hand, the low-temperature conductivity of some charge-transfer salts may even decrease with increasing pressure.[5]

Crystals of Au($dmit$)$_2$ salts oxidized in the presence of K^+, Na^+, or Li^+ ions were earlier studied under hydrostatic pressure.[6] The conductivity of K[Au($dmit$)$_2$]$_2$ crystals was about 100 S/cm at ambient pressure at room temperature. At a pressure of 1 kbar the conductivity was found to have its maximum at 130 K. However, with increasing pressure the conductivity increased and the maximum shifted to lower temperatures. At 10 kbar the conductivity increases continuously with decreasing temperature down to the lowest measured temperature of 1.5 K. No superconductivity is reported in these crystals.

We have earlier studied the conductivity and structure of Langmuir-Blodgett (LB) films of tridecylmethylammonium-Au($dmit$)$_2$ (3C10-Au),[7-9] Fig. 1. These LB films, if electrochemically oxidized using $LiClO_4$, have relatively high conductivities, around 30 S/cm at room temperature. Conductivity and thermoelectric-power measurements indicated that the films consist of metallic regions separated by weakly conducting regions. Atomic-force microscopic (AFM) studies suggested crystallites or islands of the size of $\approx 1\,\mu$m.[9] It is probable that the islands in oxidized films correspond to highly conducting regions which are separated from each other by potential barriers. The thermal-fluctuation-induced-tunneling model by Sheng and coworkers[10,11] has earlier been used for explaining charge transport in heterogeneously conducting materials such as conductor-insulator composites and conducting polymers with relatively large islands, and might therefore be a good starting point for Au($dmit$)$_2$ LB films, too.

In this paper we report an extensive study of the electrical conductivity of LB films of 3C10-Au mixed with icosanoic acid. The conductivity is studied as a function

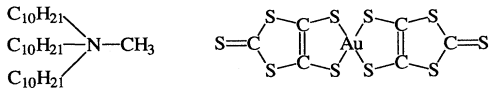

FIG. 1. Structure of tridecylmethylammonium-Au($dmit$)$_2$ (3C10-Au).

of temperature, pressure, and electric field. Early results of the pressure measurements have been published elsewhere.[12] In a previous paper[8] we explained the conductivity at ambient pressure in terms of variable-range hopping. It is found that Sheng's model gives a better description of the system. By applying pressure or a high electric field the effect of the barriers between islands can be reduced. At high temperatures the resistance of the islands starts to contribute and must be taken into account.

II. EXPERIMENT

LB films of 3C10-Au were fabricated as described earlier.[8] The monolayers were spread on a water surface from 1:1 acetonitrile:benzene solution containing a 1:1 molar mixture of 3C10-Au complex and icosanoic acid. The latter is necessary for LB film growth. Typically 20 layers were deposited on a 100-μm-thick poly(ethyleneterephtalate) (PET) substrate by the horizontal lifting method at 25 mN/m at 17 °C. The PET films were precoated with five layers of icosanoic acid and four gold electrodes having $\approx 0.3-0.5$-mm gaps for conductivity measurements. The thickness of each 3C10-Au LB layer is about 3 nm and, therefore, the overall thickness of the 20-layer films studied is 60 nm. After deposition, the films were electrochemically oxidized in 0.1 mol/l $LiClO_4$ aqueous solution.[8] The gold electrodes served as working electrodes, platinum wire being the counterelectrode. Electro-oxidation was done with constant current of 0.3–0.6 μA/3 cm^2 for 2–5 h.[13] Conductivity was checked a few times during the oxidation to avoid overoxidation, which rapidly decreases the conductivity. For example, the conductivity was found to decrease by about 50% from its maximum value for an oxidation time 20% too long. After successful oxidation the sample was rinsed with water, dried using nitrogen gas flow, and finally cut into ≈ 1-mm-wide strips for the measurements.

Pressure measurements were performed in a copper-beryllium clamp cell using Daphne oil (7373, Idemitsu Kosan Co. Ltd.) as the pressure-transferring medium.[14] The hydrostatic pressure is reported to decrease smoothly by a fixed amount of ≈ 2 kbar when the temperature is reduced from room temperature to liquid-helium temperature.[14,15] Solidification occurs at around 250 K and shifts to higher temperatures with increasing pressure. The conductivity was not affected by immersing the sample into the oil and was reversible after a pressure or temperature cycle. Still, the measurements were started as soon after electro-oxidation as possible because the films are unstable at high temperature. dc conductivity measurements were done by using the four-point technique from 3 K to room temperature with constant current of 1–10 μA. The results were not affected by starting from low pressure or starting from the highest pressure. When measuring the temperature dependence one sample was used for all pressures higher than the ambient pressure but a second strip, cut from the same PET substrate, was used to measure the ambient-pressure conductivity. Therefore, strictly speaking, the temperature dependences of pressurized samples are not directly comparable to those corresponding to ambient pressure because at the time when the latter were measured the sample had already slightly lowered its conductivity.

The electric-field dependence was measured in vacuum using the two-point technique although the four-point technique was checked to give the same results at low fields. The voltage pulses applied on the sample were in the range of 0–100 V. Short (≈ 4 μs) pulses with a low (≈ 100 Hz) repetition rate were essential to avoid Joule heating effects at high fields. The voltage across a small resistor, in series with the sample, was measured and used to calculate the current.

To obtain further information about the changes due to electro-oxidation we performed measurements of the charge-carrier mobility of the LB films prior to electro-oxidation using thin-film field-effect-transistor structures[16] which, in this study, had a channel length of 10 μm. Typically a constant drain-source voltage of -20 V was connected and the gate voltage was swept between $0 \rightarrow -20\ \text{V} \rightarrow 0$.

III. RESULTS AND DISCUSSION

The conductivity vs pressure $\sigma(p)$, at room temperature, is shown in Fig. 2. The pressure dependence is overlinear (sublinear) for samples which have a low (high) ambient-pressure conductivity σ_{amb}, respectively. The initial slope of the relative conductivity $\sigma(p)/\sigma_{amb}$ was ≈ 0.2 kbar^{-1}. Figure 3 shows the ratio $\sigma(p=10\ \text{kbar})/\sigma_{amb}$ as a function of σ_{amb}. The ratio decreases with increasing σ_{amb} and reaches a value 2.2 for the best conducting sample with $\sigma_{amb} \approx 40$ S/cm. Qualitatively similar effects have earlier been seen in bulk conducting polymers such as poly(3-alkylthiophenes).[17]

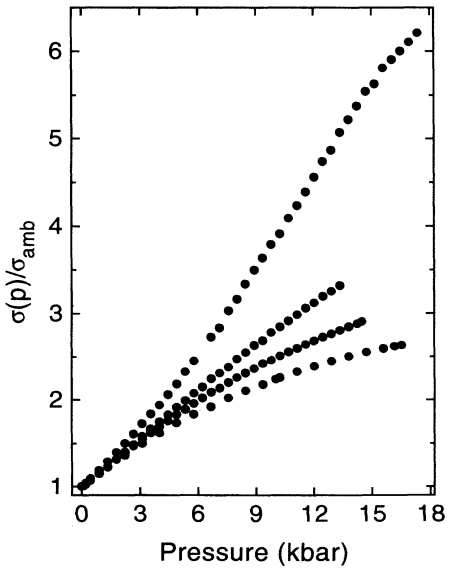

FIG. 2. Pressure-induced relative conductivity $\sigma(p)/\sigma_{amb}$ as a function of pressure at room temperature. The conductivities of the samples, σ_{amb}, are ≈ 40 (lowest curve), ≈ 20, ≈ 3, and ≈ 0.1 S/cm (highest curve).

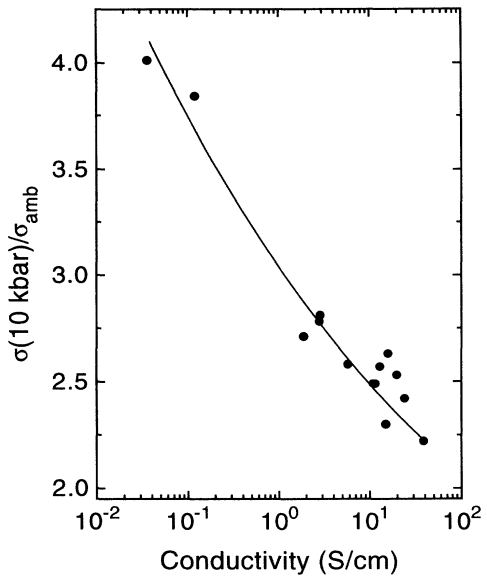

FIG. 3. Relative conductivity $\sigma(p=10\ \text{kbar})/\sigma_{amb}$ at room temperature as a function of ambient-pressure conductivity σ_{amb}. The solid line is only a guide to the eye.

The temperature dependence of the conductivity of a typical 3C10-Au LB film after electrochemical oxidation is shown in Fig. 4. As explained in Sec. II, the curves for $p>0$ are not fully comparable with the ambient-pressure curve because a new sample, with already slightly decreased conductivity and possibly some other slight differences, was used in the latter case. The smooth behavior of the conductivity in Fig. 4 is the first noticeable feature. The weak vibrations of the $\sigma(T)$ curves at 200–250 K are related to the solidification of the Daphne oil. No indication of superconductivity was seen at low temperatures. The maximum conductivity is obtained at T_{max}, which depends on pressure and the conductivity. Figure 5 shows T_{max} of highly conducting films as a function of p. For example, T_{max} of the curves in Fig. 4 varies between 194 K ($p=0$) and 86 K ($p=11.1$ kbar). Furthermore, T_{max} is smallest for samples with the highest room-temperature conductivities. At temperatures $T<T_{max}$ the conductivity-temperature coefficient $d\sigma/dT$ is positive, a behavior which is often connected to insulators or semiconductors, and at higher temperatures $d\sigma/dT$ is negative as in ordinary metals. The pressure affects both the overall conductivity and its temperature dependence. The metallic nature of the conductivity becomes enhanced at higher pressures, i.e., σ and $\sigma(T_{max})/\sigma(300\ \text{K})$ increase and at the same time T_{max} shifts to lower temperature. One can estimate from Fig. 5 by extrapolating that pressures exceeding 20 kbar could shift T_{max} to 0 K. Although the full suppression of the transition is not reached in the pressure range used, the inset of Fig. 4 shows that $\sigma(p=9.8\ \text{kbar})$ of an especially highly conducting sample stays above the room-temperature value throughout the whole temperature region measured down to 3 K. The effect of the pressure in our LB films is qualitatively similar to that observed for $K_x[Au(dmit)_2]$ crystals for $p<10$ kbar.[6] However, at a pressure of 10 kbar the metal-semiconductor transition of $K_x[Au(dmit)_2]$ crystal was fully suppressed resulting in a continuous increase of conductivity down to the lowest measured temperature of 1.5 K.

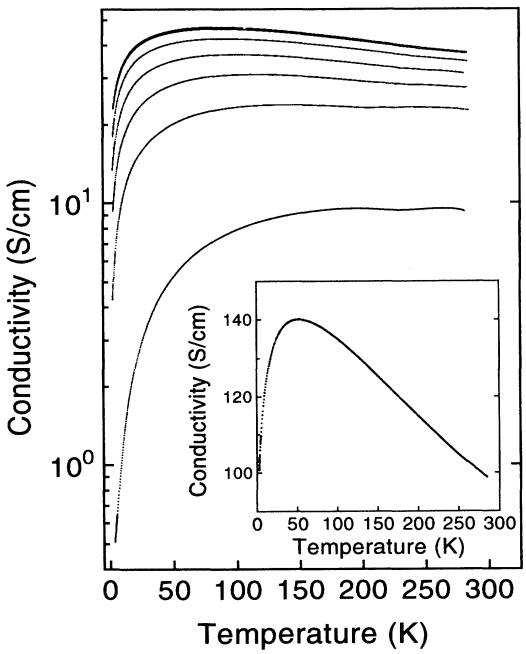

FIG. 4. Conductivity of a typical sample as a function of temperature for pressures 0 (lowest curve), 2.7, 5.0, 7.0, 9.5, 10.9, and 11.1 kbar (highest curve). A different sample from the same oxidation was used to measure the ambient-pressure conductivity. The inset shows the conductivity of the sample with the highest conductivity at $p=9.8$ kbar.

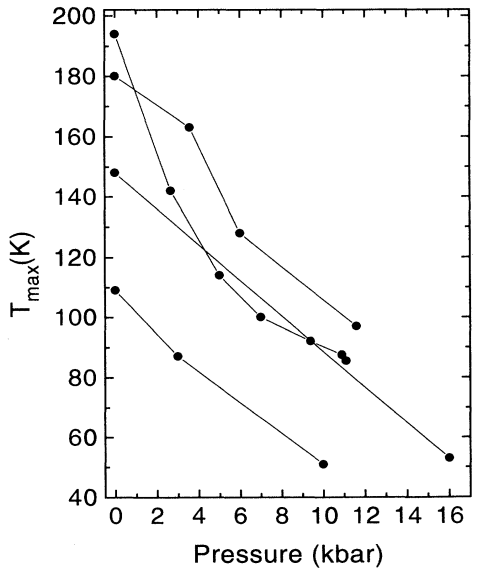

FIG. 5. Temperature at maximum conductivity T_{max}, as a function of pressure for four different highly conducting samples.

The disorder-induced metal-insulator transitions in inorganic semiconductors and conducting polymers have earlier been analyzed by studying the temperature dependence of the reduced activation energy $W=d(\ln\sigma)/d(\ln T)$.[18,19] By plotting $\ln W$ as a function of $\ln T$ and looking at the slope at low temperatures an elimination of possible conduction models for explaining the region where $d\sigma/dT>0$ can be made. The variable-range-hopping models would predict a negative slope. Figure 6 shows W vs T for a 3C10-Au LB film at ambient pressure, presented in a doubly logarithmic scale. The slope is positive for the lowest temperatures $T<10$ K strongly suggesting that the variable-range-hopping models can be disregarded. According to Ref. 18 the positive slope indicates that the samples are on the metallic side, although still in the vicinity of the metal-insulator transition, despite the fact that $d\sigma/dT$ is positive. At high temperatures a true metallic conductivity with $d\sigma/dT<0$ is observed in 3C10-Au LB films and W obtains a negative value.

The metal-insulator analysis above is relatively general and very easy to perform, and suggests that the films are not far from being metallic. However, the approach disregards the information we already have on the structure and order of the 3C10-Au LB films which, as explained above, are not "homogeneously disordered" but expected to consist of two different regions, metallic islands and less conducting barriers. While the barriers limit the conductivity, the islands may still dominate the thermoelectric power.[20] The thermoelectric power of 3C10-Au has a low value of 10–25 μV/K at room temperature and a slightly sublinear temperature dependence.[8] Although the thermoelectric-power measurements are not conclusive enough to tell which model should be employed for dc conductivity, the results are in full agreement with the existence of metallic islands in the 3C10-Au LB films.

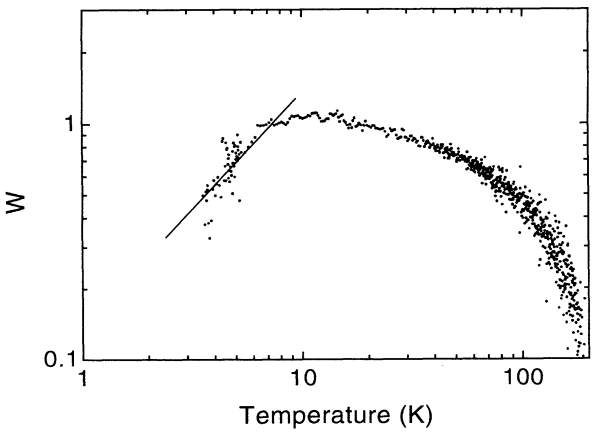

FIG. 6. Reduced activation energy $W=d(\ln\sigma)/d(\ln T)$ as a function of temperature for a sample at ambient pressure. The slope is positive below about 10 K, and W becomes negative (not shown in the figure) above 200 K. The solid line indicates a slope $d(\ln W)/d(\ln T)=1$. The results are for the lowest curve of Fig.4.

The thermal-fluctuation-induced-tunneling (TFIT) model[10,11] has been derived for a metal-island–barrier system and thus becomes a plausible explanation for $\sigma(T)$ at low temperatures. The model takes the thermal fluctuation voltage across the barriers into account and predicts that the conductivity increases with increasing temperature. Measurements of $\sigma(T)$ reported in this paper are better fitted to the TFIT model than variable-range-hopping models. For example, theoretically $d(\ln W)/d(\ln T)\rightarrow 1$ for $T\rightarrow 0$ in the TFIT model, which is in excellent agreement with the measured behavior of the ambient-pressure conductivity below about 7 K, Fig. 6. However, the simple TFIT model is not able to explain why the conductivity has a maximum. It seems probable that at high temperatures the intraisland resistance may start to contribute to the sample resistance and, as a result, $\sigma(T)$ has a maximum at $T_{\max}$ and a true metallic temperature dependence is detected at $T>T_{\max}$. The TFIT model as well as an extended model taking the intraisland resistance into account also are used in the analysis below.

First we assume that the applied voltage is fully concentrated over the barriers. The barrier potential is taken to be symmetrical, and its form assumed to be parabolic, $V(x)\approx V_0-(4V_0/w^2)x^2$, where V_0 and w are the barrier height and width, respectively ($x=0$ at the center of the junction).[10] The conductivity of the TFIT model can be written in the form

$$\sigma=\sigma_0\exp[-T_1/(T_0+T)]\,, \tag{1}$$

where the fitting parameters T_1 and T_0 can be expressed as a function of V_0, w, and barrier cross section A as follows:

$$T_1=8AV_0^2\varepsilon_0/(e^2k_Bw)\,, \tag{2}$$

$$T_0=8\sqrt{2}\hbar AV_0^{3/2}\varepsilon_0/(\pi e^2k_B\sqrt{m_e}w^2)\,. \tag{3}$$

Here ε_0 is the permittivity of vacuum, e the elementary charge, k_B the Boltzmann constant, $\hbar$ Planck's constant, and m_e the free-electron mass.

The parameters σ_0, T_1, and T_0 fitted in the low-temperature region $T=3-50$ K to the curves of Fig. 4 are given in Fig. 7. The figure indicates that σ_0 increases and T_1 decreases with increasing pressure, but T_0 remains nearly constant at $p\geq 2.7$ kbar. The data for one curve are replotted in Fig. 8 to judge the goodness of this model. The fit is excellent at low temperatures but strongly deviates from the experimental curve at high temperatures, reflecting the fact that Eq. (1) can only predict a conductivity which increases with increasing temperature.

The neglect of the intraisland resistance may be a reasonable approximation at the lowest temperatures $T\ll T_{\max}$ but completely loses its accuracy at high temperatures $T\approx T_{\max}$ or higher. A more extensive model is clearly needed to cover the whole temperature range up to room temperature and can also reveal interesting features of the transport within the islands. Assuming that the total resistance of the island-barrier system is a sum of the resistances of a barrier and an island, the total

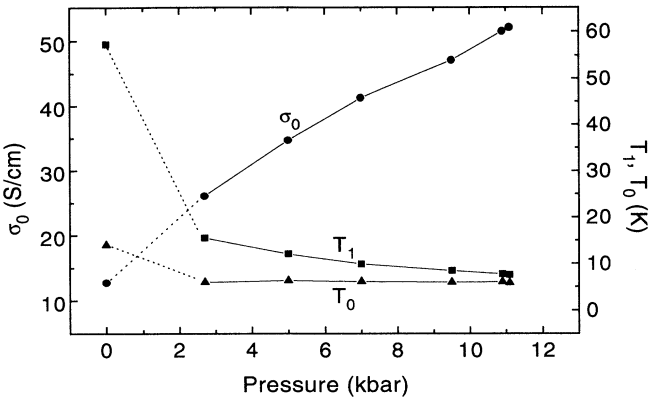

FIG. 7. Parameters σ_0, T_1, and T_0 obtained by fitting the TFIT model of Eq. (1) to the curves in Fig. 4 in the range $T \approx 3-50$ K. The solid and dotted lines are to guide the eye.

conductivity can be written in the form[20]

$$\sigma = \rho^{-1} \approx \frac{1}{f_1 \rho_{\mathrm{TFIT}} + f_2 \rho_M} . \tag{4}$$

This model will be called the "extended TFIT model" in the following text. The resistivity $\rho_{\mathrm{TFIT}} = 1/\sigma_{\mathrm{TFIT}}$ is expressed using Eq. (1). We assume here that the resistivity within a metallic island is proportional to T, i.e., $\rho_M = 1/\sigma_M = aT$ (a is a constant) which is approximately valid for normal metals at high temperatures although less accurate at low temperatures.[21]

In principle, the factors f_1 and f_2 have some temperature dependence because the islands and barriers have variation in their properties. It is still often reasonable to assume that f_1 and f_2 are temperature independent (see Ref. 20), and we adopt this approach here. At low temperatures $\rho_{\mathrm{TFIT}} \gg \rho_M$ and simple TFIT should dominate. Therefore it is natural to assume that $f_1 = 1$ which gives the extended TFIT model a correct limiting behavior equal to the TFIT model of Eq. (1) for $T \to 0$. On the other hand, for high temperatures $\sigma \to \sigma_M / f_2$, i.e., the islands dominate the transport. The factor f_2 is probably larger than unity because part of the film volume and cross-sectional area are insulating. Therefore $\sigma'_M \equiv \sigma_M / f_2$ is a lower-limit estimation of the intraisland conductivity σ_M.

Figure 9 gives the parameters obtained by fitting the extended model [Eq. (4)] to the experimental $\sigma(T,p)$ curves over the whole temperature range measured. σ_0 and typically T_0 increase while T_1 decreases with increasing pressure for $p \geq 2.7$ kbar. The values of the fitting parameters of the extended model are somewhat different from those of the simple TFIT model. The quality of the fits, see Fig. 8, was excellent at high temperatures where the assumption $\rho_M = 0$ is clearly an oversimplification. According to Fig. 9 the conductivity of the metallic islands is not strongly dependent on p for $p \geq 2.7$ kbar, and has a value $\sigma'_M \approx 100$ S/cm at 300 K while the experimental macroscopic conductivity is less than 40 S/cm. The prefactor σ_0 has pressure-dependent values which are lower than σ'_M. The ratio ρ'_M/ρ, i.e., the contribution of the islands to the sample resistance, is given in Fig. 10. We found that ρ'_M/ρ, at 300 K, increases with increasing pressure, as it should for the model to be valid. At a pressure of 11 kbar about 40% of the room-temperature resistance is due to the islands. The ratio ρ'_M/ρ at the experimental $T_{\max}$ is less variable and has a value 0.10–0.14 depending on the pressure.

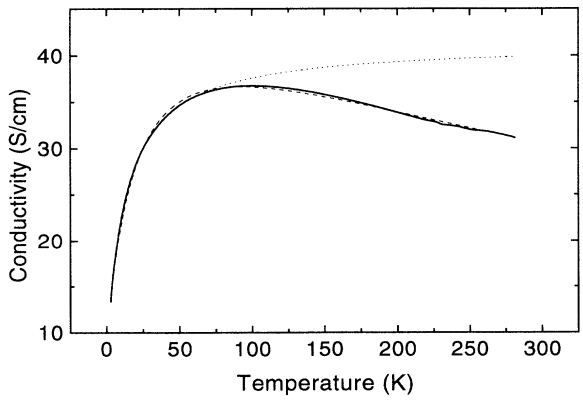

FIG. 8. Data of Fig. 4 for $p = 7.0$ kbar (thick solid line) together with the fits of the TFIT model [Eq. (1)] (dotted line) and the extended TFIT model [Eq. (4)] (dashed line).

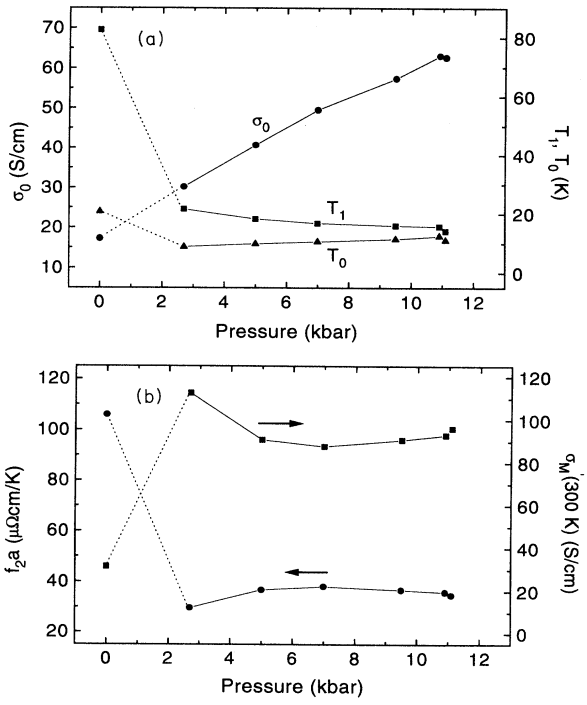

FIG. 9. Parameters obtained from fitting of the extended TFIT model [Eq. (4)] to the curves in Fig. 4 over the whole temperature range measured. (a) σ_0, T_1, and T_0 of the interisland transport. (b) $f_2 a$ of the metallic islands. The calculated value of $\sigma'_M(T = 300$ K) is also shown.

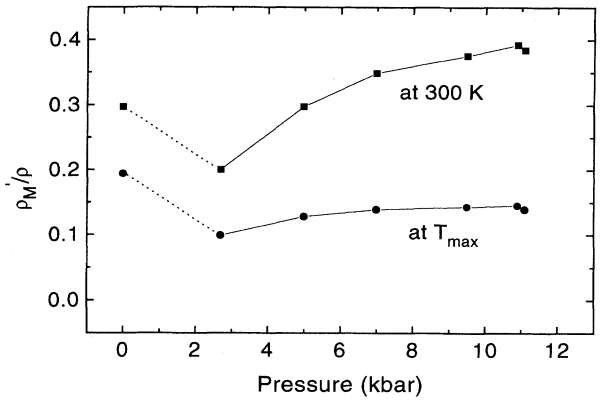

FIG. 10. Ratio ρ_M'/ρ at 300 K and at the experimental T_{max}.

To be able to calculate V_0, w, and A of the potential barriers from T_1 and T_0 one of the former has to be fixed. With AFM we have seen islands of micrometer size,[9] but it is impossible to fix barrier width or cross section based on these measurements. We found that it is possible to get an order-of-magnitude estimation of V_0 from high-field measurements.

Figure 11 shows the current as a function of applied electric field $j(E)$ at different temperatures. The current is linearly proportional to the field at $T>200$ K but overlinear at lower temperatures for fields exceeding about 1 kV/cm. We found that correct results could only be obtained by using short voltage pulses. dc measurements at high fields were unreliable, giving too large currents and easily destroying the sample. Such a behavior can be easily understood in the context of the TFIT model to be due

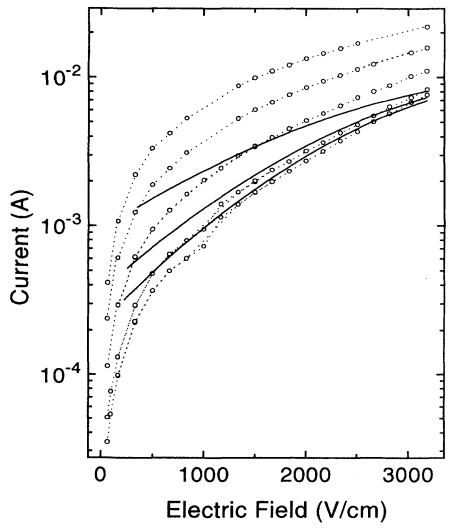

FIG. 11. Conductivity as a function of electric field at $T=11$ (lowest curve), 20, 48, 98, and 249 K (highest curve). The solid curves have been calculated for $T=10.9$, 19.8, and 47.7 K using Eq. (5) and parameters $T_1=235$ K, $T_0=50$ K, $j_0=0.010$ A, and $E_0=4700$ V/cm.

to local heating at the barriers between metallic islands.[22]

At high electric field the current in the TFIT model is given by[10,11]

$$j(E)=j_0\exp\left[-\frac{T_1}{T_0+T}\left[\frac{E}{E_0}-1\right]^2\right]. \quad (5)$$

Here E is the electric field over the barrier and $E_0=4V_0/(ew)$. The samples used for high-field measurements had a room-temperature conductivity of $\approx 10-15$ S/cm. Still, the temperature dependence of the low-field conductivity at low temperatures was stronger than that of the samples of Fig. 4 discussed earlier. These differences are due to small differences, e.g., in the oxidation level. A fit of the conductivity to Eq. (4) gave parameters $\sigma_0\approx 31$ S/cm, $T_1\approx 235$ K, $T_0\approx 50$ K, and $f_2 a\approx 71$ $\mu\Omega$ cm/K. Using these values of T_1 and T_0, we then fitted the experimental $j(E)$ measured at $T=11$ K to Eq. (5) and obtained $j_0\approx 0.010$ A and $E_{0,\mathrm{fit}}\approx 4700$ V/cm. The two other fitting curves for $T=20$ K and $T=48$ K, also shown in Fig. 11, were calculated using Eq. (5) and the same values of j_0 and $E_{0,\mathrm{fit}}$ without any free parameters. The good agreement with experiments at low temperatures strongly supports the TFIT model. For simplicity, we have not taken the island resistances into account in Eq. (5). At the lowest temperatures their effect should be small.

Since the applied voltage is concentrated at the barriers, the field at them is larger than the applied value by a factor D/w (D is the size of metallic islands). This was not taken into account in the equation for E_0 given above. Therefore, since $E_{0,\mathrm{theor}}/E_{0,\mathrm{fit}}\approx D/w$, $E_{0,\mathrm{fit}}$ is related to the barrier height and island diameter via the equation $E_{0,\mathrm{fit}}\approx 4V_0/(eD)$. Assuming, based on AFM results of Ref. 9, that $D\approx 1$ μm, a value $V_0\approx 0.12$ eV is obtained, further indicating that $w\approx 17$ Å and $A\approx 570$ Å^2. Relatively similar values were obtained by using Eq. (1), instead of Eq. (4), in the fit. These values are physically reasonable, not very different from those obtained for carbon-polyvinylchloride composite ($V_0\approx 0.2$ eV, $w\approx 75$ Å, and $A\approx 250$ Å^2),[10] or for poly(3-octylthiophene) blends ($V_0\approx 0.1-0.2$ eV, $w\approx 30$ Å, and $A\approx 1000$ Å^2).[23] In highly doped polyacetylene the barrier height is probably smaller, 4–100 meV.[11,24]

The values of T_0 and T_1 in Fig. 9, theoretically proportional to $V_0^{3/2}$ and V_0^2, respectively, indicate that the barrier height of the samples of Fig. 4 is probably less than 0.1 eV. An assumption $V_0\approx 60-80$ meV at ambient pressure is reasonable. For a barrier height of 70 meV the values of w and A are 19 Å and 620 Å^2, respectively. An additional effect comes from the pressure, because w decreases with increasing pressure which makes the barriers more penetrating. This is clearly seen as an increase of σ and a decrease of T_{max}. However, it is not clear how V_0 and A are affected by pressure. Two different limiting behaviors are therefore studied. (1) A is not dependent on pressure. This was assumed to be the case when mechanical stress was used to modulate the barriers.[25] Assuming that A has the ambient-pressure value of 620 Å^2 at all pressures, the barrier height and width would decrease from 70 meV and 19 Å ($p=0$) to 22 meV and 11

Å ($p=11$ kbar), respectively. The lowest value of V_0 is of the order of the thermal energy at room temperature ($\approx$26 meV). (2) If the compression is isotropic, A changes but A/w^2 should roughly remain constant. Then the barrier height would be nearly constant, equal to 40–50 meV at $p=2.7-11.1$ kbar. The barrier width and area would decrease from 19 Å and 620 Å^2 ($p=0$) to 7 Å and 90 Å^2 ($p=11$ kbar), respectively. The results of both approaches as well as those for constant V_0 of 70 meV for all pressures are shown in Fig. 12. If the barrier regions have a higher compressibility than the islands, the actual situation is between the two former cases.

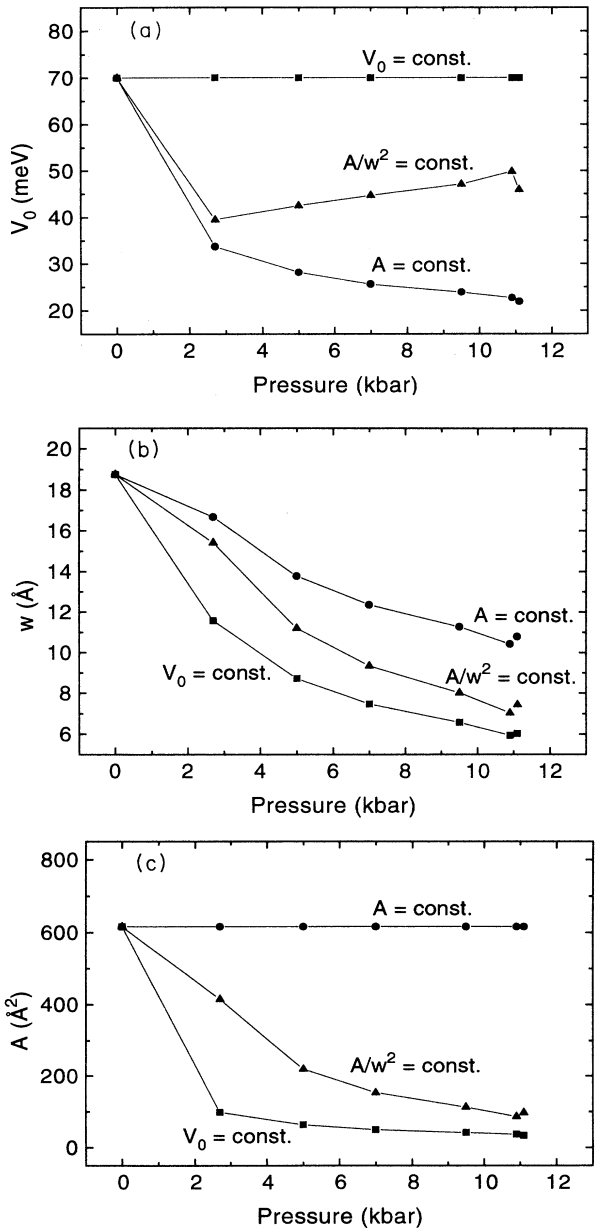

FIG. 12. Values of (a) V_0, (b) w, and (c) A calculated using different approximations: constant A of 620 Å^2, constant A/w^2 of 1.8, or constant V_0 of 70 meV.

It is worth mentioning here that the conductivity obeying Eq. (1) may also have a more simple physical interpretation.[26] A similar temperature dependence could be due to approximate interpolation between two simple mechanisms: tunneling through the barriers at $T=0$ and thermal activation of electrons over the barriers at high temperatures. The barrier height would equal $k_B T_1$, suggesting values from a few meV to about 1 meV for $p=0-11$ kbar which would indicate easy activation across the barriers even at low temperatures. The barrier widths are still relatively large, of the order of a few nanometers. Although it is not possible to completely rule out this interpretation, these barrier heights are lower than what is intuitively expected in partly disordered 3C10-Au films. The TFIT model also predicts the high-field transport correctly and has earlier been applied to many materials with success, and is therefore preferred.

The relatively high conductivity of the islands in electro-oxidized samples compared to the low conductivities in pristine samples is due to the increasing number of charge carriers and/or increasing mobilities. Assuming that there is one carrier per two Au($dmit$)$_2$ units in the metallic islands, the carrier concentration in the islands $n\approx 3\times 10^{20}$ cm^{-3} and the mobility $\mu=\sigma_M/(en)\approx\sigma'_M/(en)$ is of the order of a few cm^2/V s at room temperature. Although the estimated intraisland as well as the experimental conductivities in 3C10-Au LB films are high among organic thin films, the conductivities of normal metals are still much higher, around 10^5 S/cm.[21] The difference of a factor $\approx 10^3-10^4$ is probably mostly due to the higher number of carriers, around $10^{22}-10^{23}$ cm^{-3} in normal metals. The imperfections present in the LB films increase the scattering of the carriers, also limiting the conductivity. In fact, the room-temperature mobilities in normal metals ($\mu\approx 50$ cm^2/V s in Cu), semimetals, and inorganic semiconductors ($\mu\approx 100$ cm^2/V s in highly doped n-type Si) are typically higher than those estimated for the 3C10-Au LB films.

Preliminary studies of thin-film field-effect transistors of unoxidized Au($dmit$)$_2$ LB films (around 20 layers) indicated p-type behavior and very low field-effect mobilities. The conductivity and mobility increased reversibly if measurements were repeated several times without any setting time between them. The conductivity and mobility for the first measurements were $\sigma\approx 10^{-8}$ S/cm and $\mu_{FE}\approx 10^{-7}$ cm^2/V s, respectively. The carrier (hole) concentration $n\approx\sigma/(e\mu_{FE})\approx 10^{18}$ cm^{-3} was more constant. The carrier concentration is much lower than the value estimated for oxidized films but still relatively high considering that the films were fully unoxidized. The carriers are probably due to air oxidation because the samples were measured in air. The results indicate that the much higher conductivity after electrooxidation is due to a considerable increase of both the carrier concentration and the mobility.

IV. SUMMARY

We have measured the conductivity of LB films of tridecylmethylammonium-Au($dmit$)$_2$ as a function of

pressure, temperature, and electric field. The results of these measurements show that the conductivity can be drastically increased with pressure resulting in a more metallic temperature dependence. In the best conducting LB films the conductivity under high pressure was always above the room-temperature value down to 3 K. The temperature, pressure, and electric-field dependences of conductivity at low temperatures are explained by the thermal-fluctuation-induced-tunneling model which has been extended to take the island resistances into account. The experiments indicate that the barrier height is typically less than 0.1 eV and barrier width about 2 nm at ambient pressure. The pressure decreases the barrier width. At high temperatures and/or pressures the resistance of the islands starts to contribute to the macroscopic conductivity. Their conductivity seems to be pressure independent and has a value at least ≈ 100 S/cm at room temperature. This high value is based on a relatively high carrier mobility and carrier concentration after electro-oxidation.

ACKNOWLEDGMENTS

We thank Dr. Keizo Murata, Electrotechnical Laboratory at Tsukuba, for the guidance with the pressure measurements.

*Present address: Department of Chemistry, University of Houston, Houston, Texas 77204-5641.

[1]L. Brossard, M. Ribault, M. Bousseau, L. Valade, and P. Cassoux, C. R. Acad. Sci. Ser. II **302**, 205 (1986).

[2]L. Brossard, H. Hurdequint, R. Ribault, L. Valade, J.-P. Legros, and P. Cassoux, Synth. Met. **27**, B157 (1988).

[3]A. Kobayashi, H. Kim, Y. Sasaki, R. Kato, H. Kobayashi, S. Moriyma, Y. Nishio, K. Kajita, and W. Sasaki, Chem. Lett. **1987**, 1819.

[4]A. Kobayashi, H. Kobayashi, A. Miyamoto, R. Kato, R. A. Clark, and A. E. Underhill, Chem. Lett. **1991**, 2163.

[5]S. Tomic, D. Jerome, A. Aumuller, P. Erk, S. Hunig, and J. U. von Schutz, Synth. Met. **27**, B281 (1988).

[6]C. E. Wainwright, R. A. Clark, A. E. Underhill, I. R. Marsden, M. Allan, and R. H. Friend, Synth. Met. **41-43**, 2269 (1991).

[7]T. Nakamura, M. Matsumoto, H. Tachibana, M. Tanaka, Y. Kawabata, and Y. F. Miura, Synth. Met. **41-43**, 1487 (1991).

[8]Y. F. Miura, M. Takenaga, A. Kasai, T. Nakamura, M. Matsumoto, and Y. Kawabata, Jpn. J. Appl. Phys. **30**, 3503 (1991).

[9]M. Yumura, T. Nakamura, M. Matsumoto, Y. Kuriki, K. Honda, M. Kurahashi, and Y. F. Miura, Synth. Met. **57**, 3865 (1993).

[10]P. Sheng, E. K. Sichel, and J. I. Gittleman, Phys. Rev. Lett. **40**, 1197 (1978).

[11]P. Sheng, Phys. Rev. B **21**, 2180 (1980).

[12]Y. F. Miura, H. Isotalo, K. Kawaguchi, T. Nakamura, and M. Matsumoto, Appl. Phys. Lett. **63**, 1705 (1993).

[13]The oxidation potential was not regulated, resulting in a significant amount of leakage current during the oxidation. Therefore, it is very difficult to estimate the exact degree of oxidation from the total current.

[14]K. Murata, M. Tokumoto, H. Anzai, H. Bando, G. Saito, K. Kajimura, and T. Ishiguro, J. Phys. Soc. Jpn. **54**, 1236 (1985).

[15]H. Sato, Doctoral thesis, Kyoto University, 1993.

[16]J. Paloheimo, P. Kuivalainen, H. Stubb, E. Vuorimaa, and P. Yli-Lahti, Appl. Phys. Lett. **56**, 1157 (1990).

[17]H. Isotalo, M. Ahlskog, and H. Stubb, Synth. Met. **48**, 313 (1992).

[18]A. G. Zabrodskii and K. N. Zinoveva, Zh. Eksp. Teor. Fiz. **86**, 727 (1984) [Sov. Phys. JETP **59**, 425 (1984)].

[19]Reghu Menon, C. O. Yoon, D. Moses, A. J. Heeger, and Y. Cao, Phys. Rev. B **48**, 17 685 (1993).

[20]A. B. Kaiser, Phys. Rev. B **40**, 2806 (1989).

[21]N. W. Ashcroft and N. D. Mermin, *Solid State Physics* (CBS Publishing, Tokyo, 1981).

[22]E. K. Sichel, J. I. Gittleman, and P. Sheng, Phys. Rev. B **18**, 5712 (1978).

[23]E. Punkka, J. Laakso, H. Stubb, and P. Kuivalainen, Phys. Rev. B **41**, 5914 (1990).

[24]Y.-W. Park, A. J. Heeger, M. A. Druy, and A. G. MacDiarmid, J. Chem. Phys. **73**, 946 (1980).

[25]E. K. Sichel, P. Sheng, J. I. Gittleman, and S. Bozowski, Phys. Rev. B **24**, 6131 (1981).

[26]Th. Schimmel, D. Gläser, M. Schwoerer, and H. Naarmann, in *Conjugated Polymers,* edited by J. L. Bredas and R. Silbey (Kluwer, Dordrecht, 1991), pp. 49–111.